

1 **Short Title:** GmPTF1 modifies root growth responses to low P

2

3 **Author for contact:** Xin-Xin Li, Email: lixinxin0476@163.com; Phone: +86-0591-88260952

4 Address: Root Biology Center, Fujian Agriculture and Forestry University, Shangxiadian Road,

5 Cangshan district, Fuzhou, China

6

7 **Article Title:** GmPTF1 Modifies Root Architecture Responses to Phosphate Starvation in

8 Soybean

9

10 **Authors and Affiliations:**

11 Zhaojun Yang, Ying He, Yanxing Liu, Yelin Lai, Jiakun Zheng, Xinxin Li*, and Hong Liao

12 Root Biology Center, College of Life Sciences, Fujian Agriculture and Forestry University,

13 Fuzhou, 350002, China

14

15 **One Sentence Summary:**

16 The bHLH transcription factor GmPTF1 regulates the expression of β -expansin gene *GmEXPB2*

17 to modify root architecture, and thus promote phosphate acquisition, and biomass in soybean.

18

19 **List of Author Contributions:**

20 X.L. and H.L. supervised the experiments; Z.Y., Y.H. and Y.L. performed most of the

21 experiments; Y.L. and J.Z. provided technical assistance to Z.Y., Y.H. and Y.L.; X.L. and Z.Y.

22 designed the experiments and analyzed the data; X.L. and H.L. conceived the project and wrote

23 the article with contributions of all the authors.

24

25 **Funding Information:**

26 This work was financially supported by grants from the China National Key Program for Research

27 and Development (2016YFD0100700), the National Natural Science Foundation of China

28 (31601814), and the China Postdoctoral Science Foundation (2016T90592).

29

30 * **Corresponding Author Email:** lixinxin0476@163.com

31

32 **ABSTRACT**

33 Though root architecture modifications may be critically important for improving phosphorus (P)
34 efficiency in crops, the regulatory mechanisms triggering these changes remain unclear. In this
35 study, we demonstrate that genotypic variation in *GmEXPB2* expression is strongly correlated
36 with root elongation and P acquisition efficiency, and enhancing its transcription significantly
37 improves soybean yield in the field. Promoter deletion analysis was performed using six 5'
38 truncation fragments (P1-P6) of *GmEXPB2* fused with the *GUS* reporter gene in transgenic hairy
39 roots, which revealed that the P1 segment containing 3 E-box elements significantly enhances
40 induction of gene expression in response to phosphate (Pi) starvation. Further experimentation
41 demonstrated that GmPTF1, a bHLH transcription factor, is the regulatory factor responsible for
42 the induction of *GmEXPB2* expression in response to Pi starvation. In short, Pi starvation induced
43 expression of *GmPTF1*, with the GmPTF1 product not only directly binding the E-box motif in
44 the P1 region of the *GmEXPB2* promoter, but also activating *GUS* expression in a dosage
45 dependent manner. Further work with soybean transgenic composite plants showed that, altering
46 *GmPTF1* expression significantly impacted *GmEXPB2* transcription, and thereby affected root
47 growth, biomass and P uptake. Taken together, this work identifies a novel regulatory factor,
48 GmPTF1, involved in changing soybean root architecture through regulation the expression of
49 *GmEXPB2*. These findings contribute to understanding the molecular basis of root architecture
50 modifications in response to P deficiency, and, in the process, suggest candidate genes and a
51 promoter region to target for improving soybean yield through molecular breeding of P efficiency.

52

53 **Key words:** *GmEXPB2*, *GmPTF1*, Pi starvation, promoter deletion, E-box, root architecture,
54 soybean

55

56

57 INTRODUCTION

58 Phosphorus (P) is an essential mineral nutrient for plant growth and development. As a key
59 structural component of biomolecules such as nucleic acids, proteins, and phospholipids, P is
60 involved in multiple metabolic and biosynthetic processes required for the functioning of plant
61 cells. Although the total amount of P in a given soil may be high, phosphate (Pi), which is the
62 preferred form for assimilation, typically moves slowly through diffusion in the soil solution after
63 being released from largely unavailable forms fixed to soil particles in aluminum-P, iron-P, and
64 calcium-P bonds (Kochian et al., 2004; Rausch and Bucher, 2002). Low P availability significantly
65 limits crop yields, and thus stands as a worldwide constraint for crop growth and productivity.
66 Insights gained from better understanding the genetic and molecular mechanisms underlying plant
67 adaptations to P deficiency, therefore, promise to spur development of smart crop cultivars that
68 produce well in a range of P availability conditions through optimization of P utilization efficiency
69 (Tian et al., 2012).

70 Plants have evolved a variety of complex responses and adaptations to P deficiency (Muneer
71 and Jeong, 2015; Panigrahy et al., 2009). Notable examples include increasing accumulation of
72 starch and anthocyanin (Chen et al., 2018; Leong et al., 2018; Wang et al., 2015), changing of root
73 morphology and architecture (Gutierrez-Alanis et al., 2018; Li et al., 2016; Suen et al., 2018),
74 enhancing Pi transport activity (Gu et al., 2016; Wang et al., 2017), and inducing endogenous and
75 secreted phosphatases and RNases (Liang et al., 2002; Peng et al., 2018; Tian et al., 2014; Wang et
76 al., 2009).

77 As one of the least available macronutrients, with very low mobility and high fixation in soils
78 (Clarkson, 1981), Pi acquisition by plants often relies on the ability of root systems to most
79 effectively explore the soil. The heterogenous distribution of Pi observed in many soils has led to
80 discovery of plants with shallow root architectures from a soybean core collection, which provides
81 an advantageous spatial frameworks for acquiring P from the P-rich topsoil (Zhao et al., 2004).
82 Hence, root system architecture may be a critical component of efficient P acquisition in plants.
83 Support for this model arises from multiple reports of Pi starvation stimulating the formation and
84 emergence of lateral roots and root hairs (Bates and Lynch, 1996; Gaume et al., 2001; Williamson
85 et al., 2001). In certain plant species, the formation of proteoid or cluster roots is another special
86 type of root architectural adaptive response to P deficiency (Neumann and Martinoia, 2002; Zhou

87 et al., 2008). Despite numerous reports of plants responding to Pi starvation with alterations in
88 root morphology, the signaling and transcriptional regulation networks mediating these responses
89 remain largely unknown.

90 Many genes involved in remodeling plant root system architecture in response to Pi starvation
91 have been identified in a variety of plant species since the mid-aughts. For example, a diverse
92 collection of transcription factors (TFs), including ZAT6, SIZ1, ARF7, ARF19, bHLH32 and
93 WRKY75 from *Arabidopsis* (Chen et al., 2007; Devaiah et al., 2007a; Devaiah et al., 2007b;
94 Huang et al., 2018; Miura et al., 2011), OsMYB5P and OsPHR2 from rice (Wu and Wang, 2008;
95 Yang et al., 2018), and TaZAT8 from wheat (Ding et al., 2016), have been identified as playing
96 critical roles in modifying root architecture in response to P deficiency. Interestingly, a large
97 fraction of the identified Pi response regulators are members of the basic-helix-loop-helix (bHLH)
98 family of transcription factors with their N-terminal basic region and a helix-loop-helix region (Li
99 et al., 2006; Toledo-Ortiz et al., 2003). Several bHLH proteins have been shown to bind to E-box
100 (CANNTG) *cis*-regulatory elements in the promoter regions of transcriptionally regulated
101 downstream genes (Ito et al., 2012; Massari and Murre, 2000).

102 Several bHLH transcription factors associated with P deficiency responses have been
103 discovered and characterized as regulators of root architecture remodeling in multiple crop species.
104 In maize, the bHLH family member ZmPTF1 improves low Pi tolerance through regulation of
105 carbon metabolism and root growth (Li et al., 2011). Recently, this gene, which binds to G-box
106 (CACGTG) type E-box elements (Atchley et al., 1999; Massari and Murre, 2000), was
107 associated with drought tolerance and found within the promoter regions of multiple drought
108 stress responsive genes (Li et al., 2019). In rice, overexpression of *OsPTF1*, a bHLH transcription
109 factor, significantly promoted increases in total root length and root surface area, which resulted in
110 enhancement of Pi acquisition in comparisons with wild-type counterparts. Microarray analysis
111 has further revealed a large set of Pi-starvation responsive genes that are up-/down-regulated by
112 *OsPTF1* expression, and thus improve tolerance to Pi deprivation in rice (Yi et al., 2005). All of
113 these findings suggest that bHLH members function as critical regulatory components in
114 mediating root system architecture adaptations associated with P efficiency.

115 Soybean (*Glycine max*) is one of the most widely grown leguminous crops worldwide.
116 Production, however, is often limited by soil P availability. Previously, we cloned and

117 characterized a soybean β -expansin, *GmEXPB2*, from a Pi starvation induced cDNA library
118 constructed from a P-efficient soybean genotype (Guo et al., 2008; 2011). *GmEXPB2* appears to
119 be primarily expressed in roots and dramatically induced by Pi starvation. Overexpression of
120 *GmEXPB2* significantly promotes root elongation, and is accompanied by increases in plant
121 growth and P uptake under P deficiency growth conditions (Guo et al., 2011; Zhou et al., 2014).
122 Genetic modification of root morphology and architecture might, therefore, be effective strategies
123 for improving crop production in Pi limited soils. However, transcriptional regulators of
124 *GmEXPB2* responses to Pi starvation remain unknown.

125 In the present study, we take *GmEXPB2* as our Pi deficiency response subject. This β -expansin
126 gene is known to be critically involved in root system architecture responses to Pi starvation in
127 soybean (Guo et al., 2011). Since *GmEXPB2* is primarily expressed in roots and dramatically
128 induced by Pi starvation, its expression is likely controlled by a transcriptional factor possibly
129 binding to P responsiveness *cis*-elements. However, none of the motifs associated with P
130 efficiency to date have yet been identified and functionally analyzed in the promoter region of
131 *GmEXPB2*. To understand the molecular basis of the low P stress response and identify ideal
132 candidate promoters for transgenic breeding of P efficiency, the *GmEXPB2* promoter region was
133 analyzed by testing a set of mutants harboring a systematic series of deletions for responses to low
134 P availability. Then, the *cis*-elements identified as regulated by the transcription factor GmPTF1
135 were assayed in transgenic tobacco leaves and hairy roots. Participation of GmPTF1 in root
136 growth and its contributions to P efficiency was further confirmed in soybean transgenic
137 composite plants, as was induction of *GmEXPB2* transcription. The results presented here confirm
138 that *GmEXPB2* acts in root growth and yield responses to Pi starvation, and further demonstrates
139 that this vital component of P efficiency in soybean is activated by the bHLH type transcription
140 factor GmPTF1.

141

142

143 **RESULTS**

144 **Genotypic Variation in *GmEXPB2* Expression and Association with Root Elongation and P**
145 **Acquisition Efficiency**

146 To investigate whether the genotypic variation observed for *GmEXPB2* expression is associated
147 with root elongation and P efficiency, 111 genotypes from a soybean core collection (Zhao et al.,
148 2004) were classified into three groups according to the relative expression level of *GmEXPB2* in
149 roots under -P conditions. These were labeled group I, II and III with low, intermediate and high
150 expression levels of *GmEXPB2*, respectively. We discovered that the root length and P acquisition
151 efficiency varied among these groups, with group III genotypes exhibiting the highest expression
152 of *GmEXPB2*, as well as, the longest roots and highest P contents of any of the three groups (Fig.
153 1). This result suggests that enhancement of *GmEXPB2* expression might contribute to root
154 growth and improvement of P efficiency.

155

156 **Overexpression of *GmEXPB2* Significantly Improves Soybean Yield through Promotion of**
157 **Root Growth and P Uptake**

158 We further performed field trials to evaluate the effects of *GmEXPB2* expression on soybean yield.
159 In these experiments, overexpression of *GmEXPB2* (OE) significantly improved soybean growth
160 and yield (Fig. 2A). In comparisons with wild type (WT) plants, three OE lines produced 12.1,
161 23.8 and 30.4% increases in pod number (Supplemental Fig. S1A), 12.1, 20.7 and 24.4% increases
162 in seed number (Fig. 2B), 18.1, 25.5 and 27.6% increases in grain weight (Fig. 2C), and 10.0, 7.9
163 and 5.2% increases in 100 grain weight (Supplemental Fig. S1B).

164 Further investigation of how *GmEXPB2* expression affects root growth and P efficiency was
165 conducted with three OE lines of *GmEXPB2* and WT plants grown in pots to the R5 stage (Fig.
166 2D). After confirming the presence of the *bar* gene through qualitative PCR, accumulation of
167 *GmEXPB2* mRNA was monitored in leaves RT-qPCR. In these tests, expression of *GmEXPB2* was
168 3.54, 5.71, and 2.33-fold higher in the three OE transgenic lines than in WT plants (Supplemental
169 Fig. S2). Overexpression of *GmEXPB2* significantly promoted soybean root elongation and thus P
170 acquisition efficiency. Relative to WT plants, the overexpression of *GmEXPB2* led to 17.2%,
171 31.4%, and 74.9% increases in total root length, along with 46.9%, 40.5%, and 69.0% increases in
172 P content (Fig. 2, E and F). These results suggest that increasing *GmEXPB2* expression improves

Figure 1.

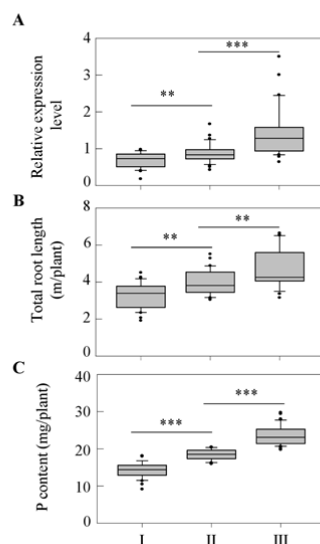


Figure 1. Association of *GmEXPB2* expression levels observed across a soybean core collection with P acquisition efficiency and root growth. The 111 observed soybean genotypes were categorized into three groups according to *GmEXPB2* transcription in roots under low P conditions. I, II, and III represent lower, intermediate, and higher expression level categories of *GmEXPB2*, respectively. P acquisition efficiency was calculated as total P content per plant. Asterisks represent significant differences between groups for the same tissue in the Student's *t* test (**: $0.001 < P \leq 0.01$, ***: $P \leq 0.001$).

173 P efficiency through regulation of adaptive changes in root system architecture, which ultimately
174 leads to increases in soybean yield in field.

175

176 **Phosphorus Availability Regulates *GmEXPB2* Expression in Different Tissues**

177 Previous studies have demonstrated that *GmEXPB2* expression is not only involved in root system
178 architecture responses to Pi starvation (Guo et al., 2011), but also improves nodulation regardless
179 of P availability (Li et al., 2015). To characterize the temporal and spatial patterns of *GmEXPB2*
180 expression in response to Pi starvation, roots, nodules and leaves were collected from plants
181 grown in P deficient or sufficient conditions and separately assayed for *GmEXPB2* transcription.
182 The results clearly show that *GmEXPB2* transcripts were predominantly localized to roots and
183 were up-regulated by P deficiency (Fig. 3A). At 7 days after inoculation (DAI), *GmEXPB2* was
184 most abundantly expressed in nodules, followed by bulk roots, but not in leaves. Then, by 14 DAI,
185 *GmEXPB2* expression was significantly enhanced in roots, especially under Pi deficiency
186 conditions, as well as, in nodules. These results confirm that *GmEXPB2* is indeed involved in
187 nodule development during early stages of organogenesis (Li et al., 2015). Plus, we reach the
188 additional conclusion here that *GmEXPB2* also appears to primarily participate in adaptive

Figure 2.

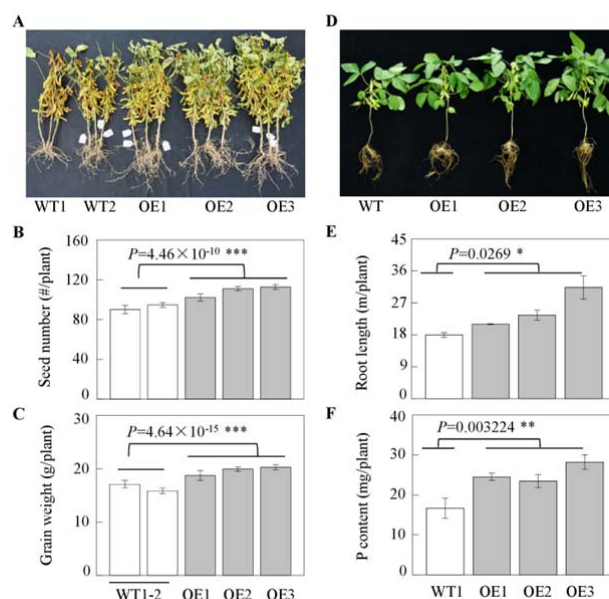


Figure 2. Overexpressing *GmEXPB2* significantly improved soybean root growth and P acquisition efficiency in a soil pot experiment, as well as, yield in a field trial. A, Growth performance. B, Total root length. C, Plant P content. D, Photograph showing soybean growth performance in a field trial. E, Seed number. F, Grain weight. Total root length and plant P content were measured at the R5 stage. WT: wild-type plants; OE: *GmEXPB2* overexpression lines. Data are means of 4 biological replicates with SE in the pot experiment, and means of 40-90 independent plants with SE in the field trial. Asterisks represent significant differences between groups in the Student's *t* test (*: $0.01 < P \leq 0.05$, **: $0.001 < P \leq 0.01$, ***: $P \leq 0.001$).

189 changes of roots responding to P deficiency, especially under long term Pi deficiency conditions.

190 Further tissue localization of *GmEXPB2* transcripts in soybeans subjected to P deprivation was
 191 conducted using GUS staining of soybean transgenic composite plants carrying the promoter
 192 region of *GmEXPB2* fused to the β -glucuronidase (GUS) reporter gene (*proGmEXPB2::GUS*)
 193 grown under Pi starvation conditions (Fig. 3B). Consistently, *GmEXPB2* reporter expression was
 194 significantly induced in roots by P deficiency conditions at 14 DAI relative to 7 DAI. Meanwhile,
 195 in nodules, GUS staining from the *proGmEXPB2::GUS* construct was strongest during early
 196 development at both 7 and 14 DAI. Taken together, these results indicate that *GmEXPB2* might
 197 play distinct roles in different tissues, with regulation of root growth responses to limited Pi
 198 availability predominating over participation in nodule development.

199

200 Identification of P Responsive Regulatory Segments of the *GmEXPB2* Promoter Region in 201 Transgenic Soybean Composite Plants

202 To characterize functional components of the *GmEXPB2* promoter, six deletion fragments were

Figure 3.

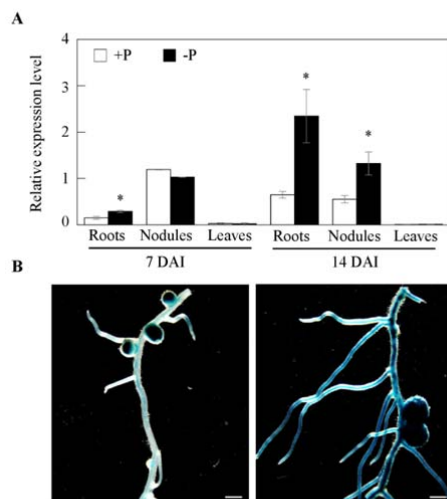


Figure 3. Regulation of *GmEXPB2* expression by P supply. A, The expression of *GmEXPB2* in roots, leaves, and nodules was determined at 7 and 14 days after inoculation (DAI) with rhizobia under -P and +P conditions. The -P and +P treatments included 5 and 200 μM KH_2PO_4 , respectively. Data are means of 3 replicates with SE. Asterisks represent significant differences in *GmEXPB2* expression in a given tissue between -P and +P treated plants as determined in the Student's *t* test (*: $0.01 < P \leq 0.05$). B, GUS staining in transgenic hairy roots and nodules developing in -P nutrient solution. Soybean transgenic composite plants harboring *proGmEXPB2::GUS* were grown in sand culture irrigated with -N and -P nutrient solution for 7 and 14 DAI with rhizobia. Scale bar=2 mm.

203 separately fused to the *GUS* reporter gene and transferred into hairy root transformants by
204 hypocotyl injection. Promoter deletions were designated as P1 to P6, with each including different
205 lengths of promoter sequence from the translation start codon (ATG) of *GmEXPB2* (Fig. 4A). All
206 of the tested truncated promoters were able to drive *GUS* gene expression in transgenic hairy roots
207 (Fig. 4B). However, only the roots harboring P1- and P2-promoter segments exhibited obvious
208 induction of *GUS* expression in response to Pi starvation. Specifically, in response to P deprivation,
209 the respective increases in *GUS* expression and its protein activity were 3.25- and 2.83-fold for P1
210 plants, and 4.67- and 1.71-fold for P2 plants (Fig. 4, C and D). No other deletion lines exhibited
211 distinct differences in *GUS* expression/activity between -P and +P conditions. These results
212 suggest that the P1 promoter (-304 to -1 bp) region contains Pi starvation responsive elements that
213 induce *GmEXPB2* expression, while as yet unidentified repressors act on elements around 500 bp
214 upstream or more from the start codon.

215

216 ***Cis*-regulatory Elements Identified in the *GmEXPB2* Promoter**

217 In order to characterize the Pi starvation responsive *cis*-regulatory elements of the P1 promoter,
218 putative *cis*-elements were first identified in a search of the NEW PLACE database

Figure 4.

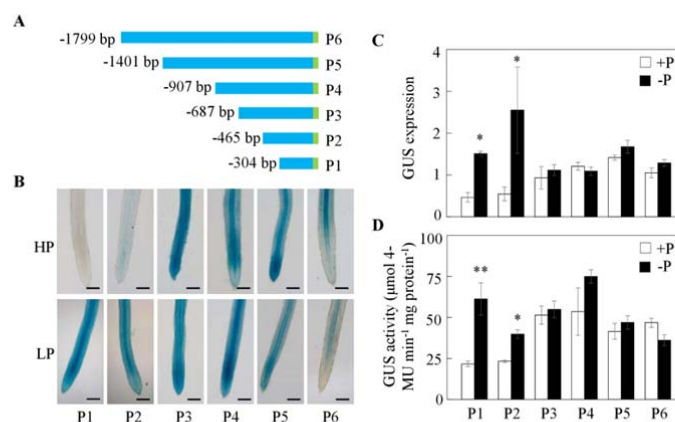


Figure 4. Deletion analysis of the *GmEXPB2* promoter. A, Schematic outlines of the truncated *GmEXPB2* promoters (P1 to P6) fused with the *GUS* reporter gene. B, *GUS* staining of hairy roots transformed with the indicated constructs under -P and +P conditions. Scale bar=1 mm. C, Relative expression of the *GUS* gene. D, Quantitative *GUS* activity analysis of the transgenic hairy roots by fluorimetric assay. Data are means of 5 replicates with SE. Asterisks represent significant differences between promoters from P1 and P2 for the same trait in Student's *t* tests (*: $0.01 < P \leq 0.05$, **: $0.001 < P \leq 0.01$).

219 (<https://www.dna.affrc.go.jp/PLACE/?action=newplace>). This returned a total of 40 bonding sites
 220 distributed unequally throughout the 304 bp upstream region of *GmEXPB2* (Supplementary table
 221 S3). Among these identified putative *cis*-elements, four are known for tissue-specific gene
 222 expression including ROOTMOTIFTAPOX1 (AATAT), RHERPATEXPA7 (ACGTGA),
 223 NODCON1GM/OSE1ROOTNODULE (ATCTTT) and POLLEN1LELAT52 (AGAAA), with
 224 root, root hair, nodulin and pollen specific motifs, respectively (Elmayan and Tepfer, 1995;
 225 Filichkin *et al.*, 2004; Kim *et al.*, 2006; Stougaard *et al.*, 1990). Several environmental
 226 stress-related motifs were also found in the P1 promoter. For example, ACGTATERD1 is required
 227 for etiolation-induced expression (Simpson *et al.*, 2003), while GATABOX and
 228 GT1CONSENSUS are mainly light-responsive regulatory elements (Rubio-Somoza *et al.*, 2006;
 229 Zhou, 1999), and MYBCORE is chiefly responsive to water stress (Urao *et al.*, 1993). In addition,
 230 three EBOXBNNAPA/MYCCONSENSUSAT/MYCATRD22 (E-box, CANNTG) motifs were
 231 identified at positions 208, 215 and 251 of the *GmEXPB2* upstream sequence (Supplementary
 232 table S3; Fig. 5A). The E-box sequence can bind basic-helix-loop-helix (bHLH) type transcription
 233 factors, and GmPTF1, a bHLH family member, is a known mediator of tolerance to Pi deprivation
 234 in soybean (Li *et al.*, 2014; Massari and Murre, 2000). In this context, GmPTF1 can be considered

Figure 5.

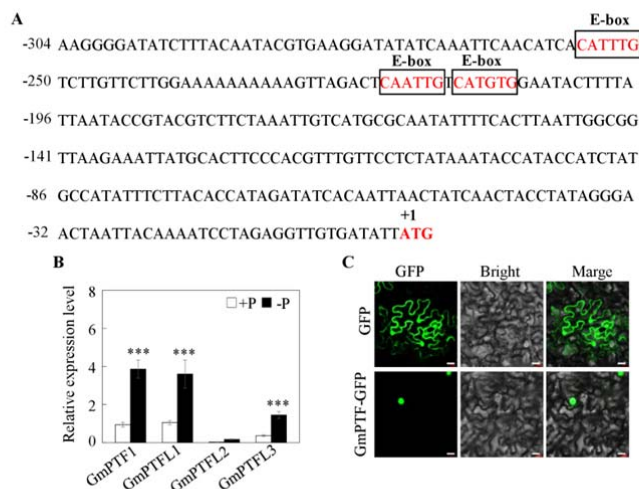


Figure 5. E-box elements in the promoter of *GmEXPB2* and putative regulatory transcription factors in soybean. A, Relative positions of the E-boxes. The translational start codon ATG was assigned position +1, and the numbers flanking the sequences of the *GmEXPB2* promoter fragments were counted from there. The E-boxes are indicated within black rectangles. B, Transcripts of *GmPTFs* in soybean roots growing under -P and +P conditions. Data are means of 5 replicates with SE. Asterisks represent significant differences between -P and +P for the same gene in the Student's *t* test (***: $P \leq 0.001$). C, Subcellular localization of GmPTF1 fused to GFP in tobacco cells. Cells were observed by green GFP fluorescence of the GmPTF1 protein (GmPTF1-GFP) with a GFP empty vector driven by 35S included as control vectors. Scale bar=100 μ m.

235 as a candidate regulating factor of soybean root architecture modification responses to Pi
 236 starvation, with responses arising primarily via transcriptional regulation of *GmEXPB2*.

237

238 **Characterization of *GmPTF* Genes and Subcellular Localization of GmPTF1**

239 Although GmPTF1 is known as a homologue of OsPTF1 that was isolated from soybean years ago
 240 (Li et al., 2014), any functionality of this gene in soybean responses to Pi starvation remains
 241 largely unclear. Here, we first quantified the extent of the GmPTF family in the soybean genome
 242 through a search of the phytozome website (<http://www.phytozome.net/>). This returned 170
 243 *GmbHLH* genes in the soybean genome. They are unevenly distributed on all chromosomes from
 244 1 to 20. A phylogenetic tree was further constructed by neighbor-joining analysis in MEGA 4.1 to
 245 determine the evolutionary relationships among the GmbHLHs family members (Supplementary
 246 Fig. S3). This demonstrated that soybean GmbHLH proteins sort into six distinct groups. Most of
 247 the previously tested GmbHLHs belong to group III, which includes 42 of the 170 bHLH
 248 members. GmPTF1 (Glyma19G143900) and its three homologs are also group III bHLHs.

249 To elucidate how this subset of GmPTF1 homologs respond to P deficiency, RT-qPCR analysis
 250 was carried out using total RNA from 25 d-old roots (Fig. 5B). Other than *GmPTFL2*, which was

251 barely detected in either P treatment, the remaining GmPTF1 homologs, *GmPTF1*, *GmPTFL1* and
252 *GmPTFL3*, were significantly up-regulated by more than 4.1-, 3.4- and 3.9-fold, respectively, in
253 response to Pi starvation. Given that *GmPTF1* exhibited the strongest response to Pi deprivation,
254 and that previous research suggests that *GmPTF1* contributes to tolerance of Pi starvation in
255 soybean (Li *et al.*, 2014), *GmPTF1* was selected as candidate gene for further study.

256 To define the subcellular localization of GmPTF1, tobacco leaves were infiltrated with
257 *agrobacterium tumefaciens* harboring a GmPTF1-GFP fusion. In contrast to control expression of
258 GFP alone, which distribute throughout the nucleus and cytosol, the GFP signal derived from the
259 fusion was exclusively confined to the nucleus (Fig. 5C). This is consistent GmPTF1 acting as a
260 transcription factor in nucleus where it might regulate downstream gene transcription.

261

262 **Dosage Effects of E-box Elements in the *GmEXPB2* Promoter**

263 Since GUS activity was significantly enhanced by Pi starvation of plants with the P1 promoter
264 containing three E-box elements, and with *GmPTF1* known as an E-box binding transcription
265 factor, the effects of *GmPTF1* expression on *GmEXPB2* promoter driven GUS activity were
266 investigated in an *Agrobacterium*-mediated co-transient assay performed in tobacco leaves (Fig. 6).
267 The P1 promoter was further truncated and named pro1 (-213 to -1) and pro2 (-220 to -1),
268 harboring one and two E-boxes, respectively (Fig. 6A). Although *GUS* was expressed with all
269 three promoters, *GmPTF1* only up-regulated *GUS* in co-transgenic tobacco leaves also harboring
270 pro2::*GUS* or P1::*GUS* (Fig. 6B). Transcription of the *GUS* gene and GUS activity itself exhibited
271 respective increases of 49% and 133% for P1, and 48% and 102% for pro2 when co-transformed
272 with *GmPTF1* in tobacco leaves (Fig. 6, C and D). In short, there appears to be a dosage effect of
273 E-boxes on the transcription of *GmEXPB2* regulated by GmPTF1. At least two E-boxes are
274 necessary for *GmEXPB2* expression to be altered by GmPTF1. Three E-boxes may promote more
275 responsive *GmEXPB2* expression than two.

276 To further confirm the effects of *GmPTF1* on P1 promoter mediated GUS activity, three
277 expression vectors containing E-boxes modified from the *GmEXPB2* promoter were constructed
278 and investigated (Fig. 6E). Interestingly, GUS staining was obviously detectable in all tobacco
279 leaves containing *GUS* fused to a *proI*, *proII*, or *proIII* promoter (Fig. 6F). However, GUS activity
280 was induced by *GmPTF1* expression only in leaves co-transformed with proI::*GUS*.

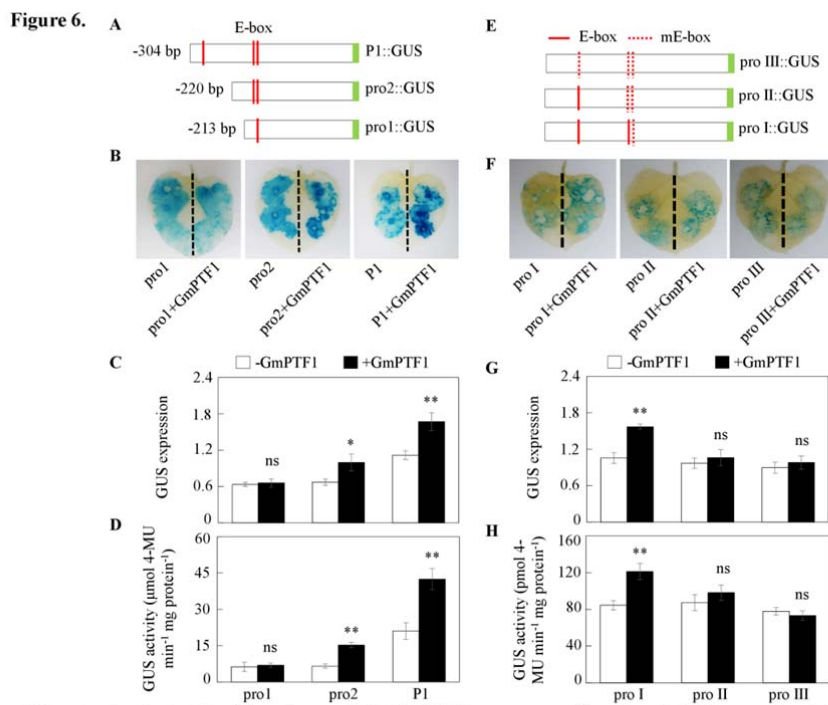


Figure 6. Functional analysis of the E-box elements in the *GmEXPB2* promoter as affected by *GmPTF1* expression. A, Schematic outlines showing the *GmEXPB2* promoter harboring different numbers of normal (E) or mutated E-boxes (mE-box). B and F, GUS staining of tobacco leaves. C and G, Relative expression of the *GUS* gene. D and H, Quantitative GUS activity analysis of transgenic tobacco leaves in fluorimetric assays. Data are means of 6 replicates with SE. Asterisks represent significant differences between promoters with different numbers of E-boxes for the same trait in the Student's *t* test (*: $0.01 < P \leq 0.05$, **: $0.001 < P \leq 0.01$). ns, Not significant at the $P=0.05$ threshold.

281 Co-expression of *proI* and *GmPTF1* led to 48.7% and 43.4% increases in *GUS* expression and its
 282 protein activity, respectively (Fig. 6, G and H). Together, these results suggest that the E-box
 283 element of the *GmEXPB2* promoter is required for *GmPTF1* activation, and increasing the number
 284 of E-box elements in the *GmEXPB2* promoter may boost the expression of the regulated gene.

285

286 **Alteration of *GmPTF1* Expression Influences Transcription of *GmEXPB2*, and Thereby** 287 **Promotes Root Architecture Modifications in Transgenic Soybean Composite Plants**

288 In order to better understand whether *GmPTF1* expression might affect the transcription of
 289 *GmEXPB2*, and thus root growth in soybean plants, *GmPTF1* overexpression and RNA
 290 interference lines (OE and Ri lines) of transgenic composite plants were generated. The quality of
 291 gene transformation in transgenic hairy roots was checked through GFP fluorescence microscopy
 292 and RT-qPCR analysis. After selecting transgenic hairy roots under a microscope (Supplementary
 293 Fig. S4), one transgenic hairy root per plant was used for further study. In RT-qPCR analysis,
 294 transcription of *GmPTF1* was 49.8 times higher in OE and 1.87 times lower in Ri plants than that

Figure 7.

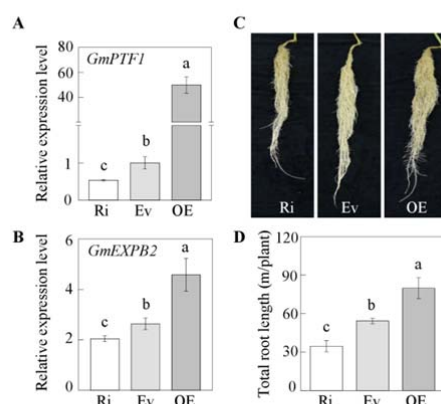


Figure 7. *GmPTF1* regulation of root growth acting through effects on *GmEXPB2* expression in transgenic composite soybean plants. A, *GmPTF1* expression in hairy roots. B, *GmEXPB2* expression in *GmPTF1* overexpressing (OE) or RNA interference (Ri) transgenic lines. C, Growth performance of hairy roots. D, Total root length. Composite soybean plants with transgenic hairy roots were grown in nutrient solution for 25 d before separately harvesting roots for analysis. Ev: control transgenic soybean hairy roots harboring empty vector. Each soybean transgenic composite plant represents one independent transgenic line, and one independent transgenic plant was considered as one biological replicate. Relative expression was normalized against the geometric mean of Ev transcription. Data are means of 5 replicates with SE. Different letters indicate significant differences between Ri or OE lines and Ev control plants for the same trait in a two-way ANOVA test ($P < 0.05$).

295 in CK lines (Fig. 7A). Moreover, altering *GmPTF1* expression significantly influenced the
296 expression of *GmEXPB2* in roots, which increased by 40.1% in OE plants, and decreased by 60.5%
297 in Ri plants when compared with CK lines (Fig. 7B). Furthermore, *GmPTF1* expression
298 significantly affected soybean root growth in transgenic composite plants, with *GmPTF1*
299 overexpressing hairy roots growing much better than control lines expressing the empty vector,
300 and suppression of *GmPTF1* producing the opposite effects (Fig. 7C). After 25 days, roots of
301 *GmPTF1* overexpressing transgenic composite plants were 47.1% longer, and those of Ri lines
302 were 36.4% shorter than control roots (Fig. 7D). These findings indicate that *GmPTF1* regulates
303 soybean hairy root growth through effects on the expression of *GmEXPB2*.

304

305 ***GmPTF1* Expression Enhances Plant Growth and P Content in Soybean Transgenic** 306 **Composite Plants**

307 Impacts of *GmPTF1* on plant growth and P efficiency were further investigated in soybean
308 transgenic composite plants. Soybean growth was enhanced in OE lines and inhibited in Ri lines
309 in comparisons with CK plants (Fig. 8A). Overexpression of *GmPTF1* led to increases of 57.9%,
310 46.2% and 30.7% in root dry weigh, plant fresh weigh and P content, respectively. Meanwhile,

Figure 8.

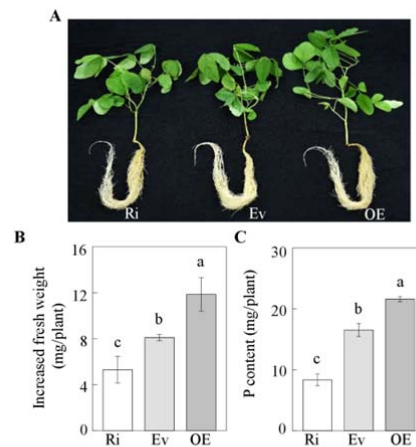


Figure 8. Effects of *GmPTF* expression on growth of soybean transgenic composite plants. A, Phenotype of composite soybean plants. B, Plant fresh weight. C, P content. Composite soybean plants with transgenic hairy roots were grown in normal nutrient solution for 25 d. Ev: control transgenic soybean nodules harboring empty vector; OE: *GmPTF* over-expressing transgenic lines; Ri: *GmPTF* RNA interference transgenic lines. Each soybean transgenic composite plant represents one independent transgenic line, and one independent transgenic plant was considered as one biological replicate. Data are means of 5 replicates with SE. Different letters indicate significant differences between Ri or OE lines and Ev control plants for the same trait in a two-way ANOVA test ($P < 0.05$).

311 suppression of *GmPTF1* resulted in a 50.5% decline in root dry weight, along with 34.6% and
312 49.5% declines in plant fresh weight and P content, respectively (Supplementary Fig. S5; Fig. 8, B
313 and C). These results indicate that regulatory effects of *GmPTF1* ultimately play important roles in
314 overall root growth and efficiency of P utilization.

315

316

317 **DISCUSSION**

318 Low phosphorus (P) availability is a major constraint on plant growth and production worldwide.
319 As the main organ involved in the acquisition of nutrients and water, roots are a logical subject of
320 research efforts aiming to incorporate plant adaptations for growth in P limited soils into crops
321 efficiently acquiring and utilizing P while maintaining high yields. Although a series of genes have
322 been reported as involved in root architecture responses to Pi starvation, to date, the transcriptional
323 regulatory mechanisms underlying these responses has remained largely unknown.
324 Overexpression of *GmEXPB2* is known to significantly enhance root growth and Pi uptake (Guo
325 et al., 2011). Here, we further evaluated how *GmEXPB2* expression influences P efficiency in
326 soybeans selected from a diverse core collection (Fig. 1). Interestingly, across the genotypes tested,
327 variation in *GmEXPB2* expression was strongly correlated with root elongation, P acquisition
328 efficiency, and resulting soybean yields in field studies (Figs. 1 and 2; Supplementary Fig. S1).
329 This indicates that *GmEXPB2* is indeed an important contributor to P efficiency and maintenance
330 of yield through modifications in root system architecture. It also suggested that *GmEXPB2* would
331 be an interesting subject in detailed exploration of transcriptional regulatory pathways guiding P
332 deprivation responses in soybean.

333 In addition to impacting P efficiency, overexpression of *GmEXPB2* also improved soybean
334 nitrogen efficiency through facilitation of nodulation, which also led to modifications in root
335 architecture regardless of P supply (Li et al., 2015). Given that *GmEXPB2* transcripts were most
336 abundant in early stages of nodule development, this gene was also tested for transcriptional
337 responses to P deficiency in roots, nodules, and leaves at 7 and 14 DAI in RT-qPCR analysis and
338 GUS staining assays (Fig. 3). Consistently, *GmEXPB2* was found to be predominantly expressed
339 in young nodules under both -P and +P conditions, but was also highly induced by Pi starvation in
340 roots. This result was also supported by the observation of GUS staining in soybean transgenic
341 composite plants carrying the *proGmEXPB2::GUS* (Fig. 3B). Further experiments in this study,
342 therefore, focus on outlining the molecular mechanisms regulating the accumulation of *GmEXPB2*
343 mRNA in roots responding to Pi starvation. Moreover, the expression of *GmEXPB2* in nodules at
344 14 DAI was significantly enhanced by P deprivation. This result stands in contrast to a previous
345 report (Li et al., 2015), in which P levels did not affect *GmEXPB2* expression in nodules at either
346 7 or 14 DAI. It is possible that *GmEXPB2* expression in nodules varies with differences in growth

347 conditions or developmental stages between the previous report and this work.

348 A number of studies have demonstrated that gene promoters are important mediators of gene
349 expression responses to stress and developmental processes (Sharma et al., 2017; Timerbaev and
350 Dolgov, 2019; Zhang et al., 2017). To investigate how *GmEXPB2* transcription in roots was
351 induced by P deprivation, a set of promoter deletions was analyzed in transgenic composite hairy
352 roots. Among tested promoter segments, the P1 and P2 sequences (304 and 465 bp upstream
353 sequences from translation start codon ATG) contained the key region for induction of *GmEXPB2*
354 expression in response to Pi starvation (Fig. 4). This result confirms histochemical expression
355 patterns reported previously in transgenic hairy roots carrying a 500 bp promoter sequence of
356 *GmEXPB2* (Guo et al., 2011), which suggests that this fragment harbors P deficiency response
357 activators. More precisely, the P1 associated strong responses in GUS activity to P deprivation
358 indicate that the main *cis*-regulatory elements responsible for P deficiency responses lie between
359 positions -304 and -1 bp.

360 Interestingly, no significant effects of P were observed in the roots of P3-P6 (587-1799 bp)
361 plants (Fig. 4). An as yet unknown low P response inhibitor might be located within the 587 to
362 1799 bp sequence shared by P3-P6. This would allow for transcription of *GmEXPB2* to be
363 influenced by multiple competing stimuli and fine tuned for a range of conditions. This is in
364 accordance with the model of a promoter region as a collection of diverse transcription factor
365 binding sites coordinating specific responses to complex sets of stimuli that may include hormonal,
366 physiological, or environmental cues (Wray et al., 2003). Given the potential complexity of
367 signals impacting the *GmEXPB2* promoter, a comprehensive description of the mechanisms
368 guiding *GmEXPB2* responses to Pi starvation at the transcriptional level requires further study.

369 Many studies have also documented the involvement of *cis*-regulatory elements in a variety of
370 regulatory networks adapted to mediate responses to fluctuating physiological and environmental
371 conditions (Hanifah et al., 2018; Kim et al., 2006; Rawat et al., 2005). In one relevant example,
372 the R2R3 MYB transcription factor PHR1 and its homologs appear to play central roles in P
373 signaling and Pi homeostasis (Bari et al., 2006; Chiou and Lin, 2011; Liang et al., 2013; Sun et al.,
374 2016; Xue et al., 2017). PHR1 binds to the P1BS element (GNATATNC) in the promoter region of
375 multiple Pi starvation induced genes, which activates gene expression (Franco-Zorrilla et al., 2004;
376 Rubio et al., 2001). Site-specific mutation or deletion of the P1BS element in the promoter region

377 abolished the transcription of a number of P responsive genes (Karthikeyan *et al.*, 2009;
378 Oropeza-Aburto *et al.*, 2012).

379 In the current study, no P1BS elements were found in the 304 bp or 2 kb promoter fragments of
380 *GmEXPB2*, while the three E-box elements described herein were closely associated at positions
381 208, 215, and 251 bp upstream of the *GmEXPB2* start codon (Supplementary Table S3; Fig. 5A).
382 bHLH transcription factors are known to bind to E-box sequences (Ito *et al.*, 2012; Massari and
383 Murre, 2000). While a total of 170 putative bHLH members were identified in the soybean
384 genome, *GmPTF1* displayed the largest increase of transcript levels in roots subjected to -P stress
385 (Supplementary Fig. S3; Fig. 5B). Further GUS staining and quantitative analysis in transient
386 co-transgenic tobacco leaves revealed that E-boxes were required for GmPTF1 to induce
387 transcription of *GmEXPB2*, furthermore, this induction appears to depend on the number of
388 E-boxes in a dosage-dependent manner (Fig. 6). This regulation of *GmEXPB2* by GmPTF1 was
389 confirmed in observations of *GmEXPB2* expression being up- or down-regulated in soybean
390 transgenic composite lines overexpressing or suppressing of *GmPTF1* (Fig. 7, A and B).
391 Furthermore, altering *GmPTF1* expression significantly impacted root growth, plant biomass and
392 P content (Figs. 7 and 8), which could be partially reproduced through manipulation of *GmEXPB2*
393 transcription in hairy roots.

394 In summary, the results presented here demonstrate that GmPTF1 modifies root architecture
395 responses to Pi starvation in soybean. Accordingly, we developed a schematic representation for
396 how *GmEXPB2* is involved in root growth and yield as regulated by GmPTF1 (Fig. 9). As a bHLH
397 transcription factor, GmPTF1, may recognize E-box binding sites in the promoter of *GmEXPB2*,
398 which are necessary for P responsive changes in *GmEXPB2* transcription in roots. From there,
399 downstream effects may include root elongation and root architecture modifications that allow for
400 soybean plants to acquire more P and, ultimately, improve soybean biomass and yield. In general,
401 the results described in this work will be useful for understanding the molecular regulation of
402 genes involved in tolerance to Pi deprivation through effects on root architecture. With further
403 study, this report might be useful for producing high yielding soybeans bred for enhanced
404 efficiency of P acquisition and utilization.

405

406 MATERIALS AND METHODS

Figure 9.

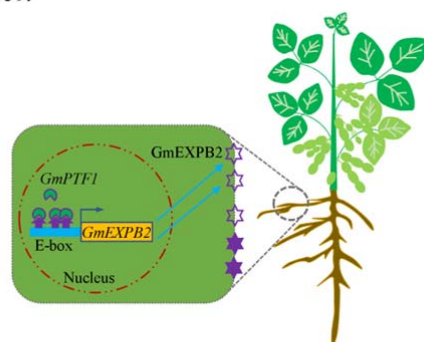


Figure 9. Hypothetical model of the *GmEXPB2* expression regulated by GmPTF1. In plants, the GmPTF1 directly enhanced *GmEXPB2* expression possibly by binding to the E-box motifs within the promoters of *GmEXPB2* to facilitate cell wall loosening, and thus modify root architecture and promote soybean yield.

407 **Plant Material and Growth Conditions**

408 Experiments in this study included plants grown in the field, pots and hydroponics. For the field
409 experiment, 111 genotypes from the soybean core collection were grown at the Boluo
410 experimental farm (E114.28°, N23.18°) of South China Agricultural University, Huizhou City,
411 Guangdong Province (Zhao et al., 2004). At the seed-filling stage, plants were harvested to
412 analyze total root length and P content.

413 To study whether overexpression of *GmEXPB2* improves soybean yield, a field experiment was
414 conducted in 2016 at the Ningxi experimental farm (23°130N, 113°810E) of South China
415 Agricultural University, Guangzhou City, Guangdong Province. The basic soil chemical properties
416 have been previously outlined (Wang et al., 2009). Seeds of wild type (WT) and three independent
417 T₄ stably transgenic lines overexpressing *GmEXPB2* (OE) were inoculated with rhizobia and then
418 grown from March to June. There were three plots of each line, and 30 seedlings in each plot.
419 Fifteen days after sowing, transgenic plants were identified in leaf painting herbicide assays.
420 Seeds were harvested at the maturation stage for recording pod and seed number, along with seed
421 weight after air-drying.

422 For the soil pot experiment, WT and three OE lines were germinated on vermiculite for 5 days

423 prior to transplanting uniform seedlings into pots. The basic soil chemical characteristics were as
424 follows: a pH of 6.46, 72.80 mg·kg⁻¹ available N, 67.49 mg·kg⁻¹ available P, and 2.7% organic
425 matter. After 15 d of growth, leaves were harvested for *bar* gene identification and real-time
426 quantitative reverse transcription PCR (RT-qPCR) analysis. At the R5 stage, plants were
427 separately sampled for total root length and P content measurements.

428 For the hydroponic experiment, seeds from the soybean core collection were surface sterilized
429 in 3% H₂O₂ for 1 min, rinsed with distilled water, and germinated in vermiculite for 7 d. Uniform
430 seedlings were cultured in soybean growth solution with low Pi supplied as 5 μM KH₂PO₄ as
431 describe previously (Qin et al., 2012). Plants were grown in growth chambers (day/night: 14 h/11
432 h, 26°C/24°C) for 14 d. Roots were harvested for RT-qPCR assays to test for a relationship
433 between *GmEXPB2* expression and root elongation and P efficiency.

434 To study temporal and spatial patterns of *GmEXPB2* expression in response to Pi starvation,
435 seeds of soybean genotype HN89 were germinated in sand prior to selecting uniform seedlings
436 after 5 d. Selected seedlings were then inoculated with highly effective rhizobium strain BXYD3
437 by immersing roots in a rhizobial suspension for 1.5 h and transplanted into a -N (530 μM N)
438 nutrient solution and treated with 5 μM (-P) or 250 μM (+P) KH₂PO₄, respectively (Li et al., 2015).
439 Nodules, roots, and entirely expanded young leaves were harvested separately 7 and 14 days after
440 inoculation (DAI). For analysis of *GmPTF1* expression in roots responding to P deficiency,
441 uniform seedlings were transplanted into hydroponic systems treated with -P and +P nutrient
442 solutions as described above for 25 days. All samples were stored at -80°C prior to RNA
443 extraction and RT-qPCR analysis.

444

445 **RNA Extraction and RT-qPCR Analysis**

446 Total high-quality RNA was extracted from soybean nodules, roots, and leaves using RNAisoTM
447 Plus reagent (Takara Bio, Otsu, Shiga, Japan) according to the manufacturer's instructions.
448 Subsequently, all RNA samples were treated with RNase-free *DNase* I (TaKaRa, Japan) to remove
449 genomic DNA. About 1 μg of RNA was used for first-strand cDNA synthesis using oligo d (T),
450 dNTPs, and MMLV-reverse transcriptase (Promega, Madison WI, USA) based on the protocol
451 from the supplier. RT-qPCR was performed using a LightCycler96 (Roche Diagnostics GmbH,
452 Germany) with the 20 μL reaction volume containing 2 μL of 1:50 diluted cDNA, 0.6 μL of

453 specific primers, 6.8 μ L of ddH₂O, and 10 μ L of Trans Start Top Green qPCR SuperMix (Trans).
454 The reaction conditions for thermal cycling were as follows: 95°C for 1 min, 40 cycles of 95°C for
455 15 s, 60°C for 15 s, and 72°C for 30 s. Fluorescence data were collected during the step at 72°C.
456 The housekeeping gene *EF-1 α* from soybean (*TefSI*, accession no. X56856) or from tobacco
457 (*Nicotiana tabacum*; *NtEF1a*, accession no. AF120093) (Schmidt and Delaney, 2010) was used as
458 a reference gene to evaluate relative expression values. Relative expression was calculated as the
459 ratio of the expression value of the target gene to that of *TefSI* or *NtEF1a* using the $2^{-\Delta\Delta CT}$ method.
460 All of the specific primers used for RT-qPCR are listed in Supplementary Table S1.

461

462 **Vector Construction**

463 To characterize functional components of the *GmEXPB2* promoter, a series of deletions upstream
464 of the translational start codon ATG were amplified by PCR. The six deletion fragments were
465 named P1 (-304 to -1), P2 (-465 to -1), P3 (-687 to -1), P4 (-907 to -1), P5 (-1401 to -1), and P6
466 (-1799 to -1). These fragments were amplified using the common reverse primers P1-6-R and the
467 forward primers P1-F, P2-F, P3-F, P4-F, P5-F, and P6-F. After digestion with *EcoRI* and *BamHI*,
468 the generated fragments were separately fused with a *GUS* reporter gene into the plant
469 transformation vector pTF102.

470 To investigate the impact of E-box *cis*-elements located in the P1 region on *GUS* reporter gene
471 expression, further deletion fragments were generated as pro1 (-213 to -1) and pro2 (-220 to -1)
472 carrying one and two E-boxes, respectively. These fragments were amplified by PCR with the
473 reverse primer P1-6-R and the forward primers pro1-F, and pro2-F. After verification by DNA
474 sequencing, the pro1 and pro2 fragments were separately cloned into the pTF102 vector as
475 described above.

476 For construction of plasmids with mutated E-box sequences, overlapping PCR was carried out
477 first with the primers pro I-F/pro II-F/pro III-F and P1-6-R, as well as P1-F and pro I-R/pro
478 II-R/pro III-R. Then, isolated sequence fragments were separately mixed and further used as
479 templates to generate pro I, pro II, and pro III fragments with one, two or three mutated E-boxes
480 amplified between the primers P1-F and P1-6-R. Among mutated fragments, the E-box sequence
481 CATGTG in pro I was modified to ACTGGT, while the sequences CAATTG and GATGTG in pro
482 II were respectively modified to AAATCG and ACTGTT, and the sequence CATTG in pro III

483 was modified to ACAAGT (highlight in blue, Supplementary Table S2).

484 To generate soybean transgenic composite plants overexpressing or suppressing *GmPTF1*, the
485 open reading frame of *GmPTF1* was amplified using the *GmPTF1*-OE-F and *GmPTF1*-OE-R
486 primers. After digestion with *Swa*I and *Bam*HI, the fragment was cloned into the binary vector
487 pFGC5941 with a 35S promoter. For the RNA interference construct, 337 bp of the *GmPTF1*
488 coding sequence was amplified using the sense orientation primers *GmPTF1*-Ri-F1 and
489 *GmPTF1*-Ri-R1 and the antisense orientation primers *GmPTF1*-Ri-F2 and *GmPTF1*-Ri-R2. The
490 PCR products were digested separately and ligated into the *Swa*I and *Bam*HI sites of the
491 pFGC5941 vector in the sense and antisense orientations. All primers used for the vector constructs
492 are listed in Supplementary Table S2, and the restriction enzyme cutting sites are underlined in the
493 corresponding primer sequences.

494

495 **Plant Transformation and Growth Conditions**

496 The hypocotyl injection method was used to generate soybean transgenic composite plants as
497 described previously (Kereszt et al., 2007), with some modifications. Hypocotyls of five-day-old
498 seedlings with unfolded cotyledons were infected with *Agrobacterium rhizogenes* strain K599
499 carrying the target gene construct. Infected plants were grown in hydroponics under high humidity
500 conditions. The main root was removed after hairy roots emerging from hypocotyl were
501 approximately 10 cm long. Each individual hairy root was checked for green fluorescent protein
502 (GFP) fluorescence to ensure the presence of the vector carrying target sequences. A single
503 transgenic hairy root was kept for further study of each construct.

504 For histochemical analysis of *GUS* expression driven by the *GmEXPB2* promoter in hairy roots
505 and nodules, transgenic soybean composite plants with hairy roots harboring *proGmEXPB2::GUS*
506 constructs (Guo et al., 2011) were inoculated with rhizobia for 1 h and then transplanted into sand
507 culture irrigated with -N (530 μ M N) and -P (10 μ M KH_2PO_4) solution for 7 and 14 days (Li et al.,
508 2015).

509 For *GmEXPB2* promoter deletion analysis, transgenic soybean composite plants with hairy
510 roots and harboring various truncated fragment constructs (P1-P6::GUS) were treated with high P
511 (+P: 200 μ M P added as KH_2PO_4) or low P (-P: 5 μ M P added as KH_2PO_4) nutrient solutions for
512 15 days. All transgenic composite soybean plants were grown in a growth chamber with a 16 h/8 h,

513 26°C/24°C, light/dark photoperiod.

514 For transformation of tobacco leaves, recombinant plasmids were introduced into
515 *Agrobacterium rhizogenes* strain EHA105 and then transiently transferred into tobacco leaves by
516 infiltration. After 2 d, transgenic leaves were harvested for GUS staining, RNA extraction and
517 fluorometric GUS assays.

518

519 **Histochemical GUS Staining and Fluorometric GUS Activity Assay**

520 For histochemical analysis of *GUS* expression, all samples including soybean transgenic hairy
521 roots and tobacco leaves were incubated in GUS staining solution containing 50 mM inorganic
522 phosphate-buffered saline (Na₂HPO₄-NaH₂PO₄ buffer, pH 7.2), 0.1% (v/v) Triton X-100, 2 mM
523 K₃Fe(CN)₆, 2 mM K₄[Fe(CN)₆]·3H₂O, 10 mM EDTA-2Na, and 2 mM
524 5-bromo-4-chloro-3-indolyl-β-d-GlcA at 37°C for 24 h. After washing three times with 75%
525 ethanol, stained samples were observed with a light microscope (Axio Imager A2m; Zeiss).

526 For the fluorometric GUS assay, transgenic soybean hairy roots and tobacco leaves were used to
527 determine GUS enzyme activity by measuring the fluorescence of 4-methylumbelliferone (4-MU)
528 produced by GUS cleavage of 4-methylumbelliferyl-β-d-glucuronide (4-MUG, Sigma, USA)
529 according to the published procedure as described previously (Jefferson, 1988; Jefferson et al.,
530 1987). Protein was extracted and quantified based on a published methods using bovine serum
531 albumin as a standard (Bradford, 1976). Fluorescence was measured with a fluorescence
532 spectrophotometer (HITACHI F-4600, Japan) at the excitation and emission wavelengths of 365
533 nm and 455 nm, respectively. GUS activity was calculated as nmol of 4-MU per minute per mg of
534 protein.

535

536 **Database Search and Molecular Sequence Analysis**

537 For analysis of *cis*-elements in the *GmEXPB2* promoter region, a 304 bp segment upstream of the
538 translational start codon ATG was searched to locate potential *cis*-acting elements using NEW
539 PLACE (<https://www.dna.affrc.go.jp/PLACE/?action=newplace>). The putative *cis*-elements are
540 listed in Supplementary Table S3. For phylogenetic tree construction of GmPTFs, the basic
541 helix-loop-helix (bHLH) transcription factors in soybean, a BLAST search was conducted at the
542 phytozome website (<http://www.phytozome.net>), which yielded 170 bHLH genes in the soybean

543 genome. Then, the phylogenetic tree was constructed based on whole protein sequence alignments
544 using ClustalX and the neighbor-joining method with 1,000 bootstrap replicates in the MEGA 4.1
545 program.

546

547 **Subcellular Localization of GmPTF1 in Tobacco Cells**

548 Subcellular localization of GmPTF1 was determined via transient expression of translational
549 fusions with GFP in tobacco leave. First, the coding region of GmPTF1 was amplified using the
550 specific primers GmPTF1-GFP-F and GmPTF1-GFP-R as listed in Supplementary Table S2. The
551 resulting fragment of *GmPTF1* was then inserted into a modified pFGC5941 vector along with a
552 *GFP* reporter gene after digestion by *AscI*. After transformation, the *Agrobacterium tumefaciens*
553 strain EHA105 harboring 35S::GmPTF1-GFP or the 35S::GFP control vector was cultured in
554 Luria-Bertani medium overnight. After centrifugation, the bacteria were re-suspended in
555 infiltration medium (10 mM MgCl₂, 10 mM MES, and 150 mM acetosyringone) to an OD600 of
556 0.45-0.55. Then, this suspension of cells containing GmPTF1-GFP constructs and the 35S empty
557 vector was used to infiltrate leaves of 3-week-old tobacco plants. Infiltrated tobacco plants were
558 grown for another 2 d and GFP florescence was observed using a confocal scanning microscope
559 (LSM880; Carl Zeiss) with 488 nm excitation and 500- to 525-nm emission filter wavelengths.

560

561 **Measurement of Plant P Content**

562 Soybean transgenic composite plants were dried at 105°C for 30 min, and then oven-dried at 75°C
563 prior to weighting. About 0.2 g of dried sample was digested and total P content was measured
564 using a continuous flow analyzer (SAN++). The resulting signals were analyzed in FlowAccess
565 software (SAN++ FlowAccess V3 data acquisition Windows software package).

566

567 **Date Analysis**

568 Results from RT-qPCR were normalized in each experiment. All data were statistically analyzed
569 using Sigma Plot to calculate means and SE. Tests for statistical significance between groups were
570 performed using Student's *t* tests or a two-way ANOVA test in SPSS (version 17.0).

571

572 **Supplemental Data**

573 **Supplemental Figure S1.** Effects of *GmEXPB2* on soybean pod number (A) and 100-grain
574 weight (B) in field trials.

575 **Supplemental Figure S2.** Molecular identification of *GmEXPB2* in stable soybean transgenic
576 lines.

577 **Supplemental Figure S3.** Phylogenetic analysis of GmPTF family members in soybean.

578 **Supplemental Figure S4.** Confirmation of RNA interference (Ri) and over-expression (OE) of
579 *GmPTF1* in soybean transgenic composite plants.

580 **Supplemental Figure S5.** Effects of RNA interference (Ri) and over-expression (OE) of *GmPTF1*
581 on root growth of soybean transgenic composite plants.

582 **Supplemental Table S1.** Gene-specific primers used for qRT-PCR analysis.

583 **Supplemental Table S2.** Gene specific primers used for *GmEXPB2* vector constructs.

584 **Supplemental Table S3.** List of *cis*-elements in the *GmEXPB2* promoter between the translation
585 start codon and 304 bp upstream of the start codon.

586

587 **Acknowledgements**

588 We thank Dr. Xiurong Wang for providing the seeds of overexpressing *GmEXPB2* soybean lines,
589 and Thomas Walk of Golden Fidelity LLC for critical reading. The authors have no conflict of
590 interest to declare.

591

592 **Figure Legends**

593 **Figure 1.** Association of *GmEXPB2* expression levels observed across a soybean core collection
594 with P acquisition efficiency and root growth. The 111 observed soybean genotypes were
595 categorized into three groups according to *GmEXPB2* transcription in roots under low P
596 conditions. I, II, and III represent lower, intermediate, and higher expression level categories of
597 *GmEXPB2*, respectively. P acquisition efficiency was calculated as total P content per plant.
598 Asterisks represent significant differences between groups for the same tissue in the Student's *t*
599 test (**: $0.001 < P \leq 0.01$, ***: $P \leq 0.001$).

600 **Figure 2.** Overexpressing *GmEXPB2* significantly improved soybean root growth and P
601 acquisition efficiency in a soil pot experiment, as well as, yield in a field trial. A, Growth
602 performance. B, Total root length. C, Plant P content. D, Photograph showing soybean growth

603 performance in a field trial. E, Seed number. F, Grain weight. Total root length and plant P content
604 were measured at the R5 stage. WT: wild-type plants; OE: *GmEXPB2* overexpression lines. Data
605 are means of 4 biological replicates with SE in the pot experiment, and means of 40-90
606 independent plants with SE in the field trial. Asterisks represent significant differences between
607 groups in the Student's *t* test (*: $0.01 < P \leq 0.05$, **: $0.001 < P \leq 0.01$, ***: $P \leq 0.001$).

608 **Figure 3.** Regulation of *GmEXPB2* expression by P supply. A, The expression of *GmEXPB2* in
609 roots, leaves, and nodules was determined at 7 and 14 days after inoculation (DAI) with rhizobia
610 under -P and +P conditions. The -P and +P treatments included 5 and 200 μM KH_2PO_4 ,
611 respectively. Data are means of 3 replicates with SE. Asterisks represent significant differences in
612 *GmEXPB2* expression in a given tissue between -P and +P treated plants as determined in the
613 Student's *t* test (*: $0.01 < P \leq 0.05$). B, GUS staining in transgenic hairy roots and nodules
614 developing in -P nutrient solution. Soybean transgenic composite plants harboring
615 *proGmEXPB2::GUS* were grown in sand culture irrigated with -N and -P nutrient solution for 7
616 and 14 DAI with rhizobia. Scale bar=2 mm.

617 **Figure 4.** Deletion analysis of the *GmEXPB2* promoter. A, Schematic outlines of the truncated
618 *GmEXPB2* promoters (P1 to P6) fused with the *GUS* reporter gene. B, GUS staining of hairy roots
619 transformed with the indicated constructs under -P and +P conditions. Scale bar=1 mm. C,
620 Relative expression of the *GUS* gene. D, Quantitative GUS activity analysis of the transgenic
621 hairy roots by fluorimetric assay. Data are means of 5 replicates with SE. Asterisks represent
622 significant differences between promoters from P1 and P2 for the same trait in Student's *t* tests (*:
623 $0.01 < P \leq 0.05$, **: $0.001 < P \leq 0.01$).

624 **Figure 5.** E-box elements in the promoter of *GmEXPB2* and putative regulatory transcription
625 factors in soybean. A, Relative positions of the E-boxes. The translational start codon ATG was
626 assigned position +1, and the numbers flanking the sequences of the *GmEXPB2* promoter
627 fragments were counted from there. The E-boxes are indicated within black rectangles. B,
628 Transcripts of *GmPTFs* in soybean roots growing under -P and +P conditions. Data are means of 5
629 replicates with SE. Asterisks represent significant differences between -P and +P for the same gene
630 in the Student's *t* test (***: $P \leq 0.001$). C, Subcellular localization of GmPTF1 fused to GFP in
631 tobacco cells. Cells were observed by green GFP fluorescence of the GmPTF1 protein
632 (GmPTF1-GFP) with a GFP empty vector driven by 35S included as control vectors. Scale

633 bar=100 μ m.

634 **Figure 6.** Functional analysis of the E-box elements in the *GmEXPB2* promoter as affected by
635 *GmPTF1* expression. A, Schematic outlines showing the *GmEXPB2* promoter harboring different
636 numbers of normal (E) or mutated E-boxes (mE-box). B and F, GUS staining of tobacco leaves. C
637 and G, Relative expression of the *GUS* gene. D and H, Quantitative GUS activity analysis of
638 transgenic tobacco leaves in fluorimetric assays. Data are means of 6 replicates with SE. Asterisks
639 represent significant differences between promoters with different numbers of E-boxes for the
640 same trait in the Student's *t* test (*: $0.01 < P \leq 0.05$, **: $0.001 < P \leq 0.01$). ns, Not significant at the
641 $P=0.05$ threshold.

642 **Figure 7.** *GmPTF1* regulation of root growth acting through effects on *GmEXPB2* expression in
643 transgenic composite soybean plants. A, *GmPTF1* expression in hairy roots. B, *GmEXPB2*
644 expression in *GmPTF1* over-expressing (OE) or RNA interference (Ri) transgenic lines. C,
645 Growth performance of hairy roots. D, Total root length. Composite soybean plants with
646 transgenic hairy roots were grown in nutrient solution for 25 d before separately harvesting roots
647 for analysis. Ev: control transgenic soybean hairy roots harboring empty vector. Each soybean
648 transgenic composite plant represents one independent transgenic line, and one independent
649 transgenic plant was considered as one biological replicate. Relative expression was normalized
650 against the geometric mean of Ev transcription. Data are means of 5 replicates with SE. Different
651 letters indicate significant differences between Ri or OE lines and Ev control plants for the same
652 trait in a two-way ANOVA test ($P < 0.05$).

653 **Figure 8.** Effects of *GmPTF* expression on growth of soybean transgenic composite plants. A,
654 Phenotype of composite soybean plants. B, Plant fresh weight. C, P content. Composite soybean
655 plants with transgenic hairy roots were grown in normal nutrient solution for 25 d. Ev: control
656 transgenic soybean nodules harboring empty vector; OE: *GmPTF* over-expressing transgenic lines;
657 Ri: *GmPTF* RNA interference transgenic lines. Each soybean transgenic composite plant
658 represents one independent transgenic line, and one independent transgenic plant was considered
659 as one biological replicate. Data are means of 5 replicates with SE. Different letters indicate
660 significant differences between Ri or OE lines and Ev control plants for the same trait in a
661 two-way ANOVA test ($P < 0.05$).

662 **Figure 9.** Hypothetical model of the *GmEXPB2* expression regulated by *GmPTF1*. In plants, the

663 GmPTF1 directly enhanced *GmEXPB2* expression possibly by binding to the E-box motifs within
664 the promoters of *GmEXPB2* to facilitate cell wall loosening, and thus modify root architecture and
665 promote soybean yield.

666

667

668

669

Parsed Citations

Atchley WR, Terhalle W, Dress A (1999) Positional dependence, cliques, and predictive motifs in the bHLH protein domain. J Mol Evol 48: 501-516.

Pubmed: [Author and Title](#)

Google Scholar: [Author Only Title Only Author and Title](#)

Bari R, Pant BD, Stitt M, Scheible WR (2006) PHO2, microRNA399, and PHR1 define a phosphate-signaling pathway in plants. Plant Physiol 141: 988-999.

Pubmed: [Author and Title](#)

Google Scholar: [Author Only Title Only Author and Title](#)

Bates TR, Lynch JP (1996) Stimulation of root hair elongation in Arabidopsis thaliana by low phosphorous availability. Plant Cell Environ 19: 529-538.

Pubmed: [Author and Title](#)

Google Scholar: [Author Only Title Only Author and Title](#)

Bradford MM (1976) A rapid and sensitive method for the quantitation of microgram quantities of protein utilizing the principle of protein-dye binding. Anal Biochem 72: 248-254.

Pubmed: [Author and Title](#)

Google Scholar: [Author Only Title Only Author and Title](#)

Chen Y, Wu P, Zhao Q, Tang Y, Chen Y, Li M, Jiang H, Wu G (2018) Overexpression of a phosphate starvation response AP2/ERF gene from physic nut in Arabidopsis alters root morphological traits and phosphate starvation-induced anthocyanin accumulation. Front Plant Sci 9, 1186.

Pubmed: [Author and Title](#)

Google Scholar: [Author Only Title Only Author and Title](#)

Chen ZH, Nimmo GA, Jenkins GI, Nimmo HG (2007) BHLH32 modulates several biochemical and morphological processes that respond to Pi starvation in Arabidopsis. Biochem J 405: 191-198.

Pubmed: [Author and Title](#)

Google Scholar: [Author Only Title Only Author and Title](#)

Chiou TJ, Lin SI (2011). Signaling network in sensing phosphate availability in plants. Annu Rev Plant Biol 62: 185-206.

Pubmed: [Author and Title](#)

Google Scholar: [Author Only Title Only Author and Title](#)

Clarkson DT (1981) Nutrient interception and transport by root systems. In: Johnson CB, editor. Physiological processes limiting plant productivity. London: Butterworths 307-314.

Pubmed: [Author and Title](#)

Google Scholar: [Author Only Title Only Author and Title](#)

Devaiah BN, Karthikeyan AS, Raghothama KG (2007a) WRKY75 transcription factor is a modulator of phosphate acquisition and root development in Arabidopsis. Plant Physiol 143: 1789-1801.

Pubmed: [Author and Title](#)

Google Scholar: [Author Only Title Only Author and Title](#)

Devaiah BN, Nagarajan VK, Raghothama KG (2007b) Phosphate homeostasis and root development in Arabidopsis are synchronized by the zinc finger transcription factor ZAT6. Plant Physiol 145: 147-159.

Pubmed: [Author and Title](#)

Google Scholar: [Author Only Title Only Author and Title](#)

Ding W, Wang Y, Fang W, Gao S, Li X, Xiao K (2016) TaZAT8, a C2H2-ZFP type transcription factor gene in wheat, plays critical roles in mediating tolerance to Pi deprivation through regulating P acquisition, ROS homeostasis and root system establishment. Physiol Plant 158: 297-311.

Pubmed: [Author and Title](#)

Google Scholar: [Author Only Title Only Author and Title](#)

Elmayan T, Tepfer M (1995) Evaluation in tobacco of the organ specificity and strength of the rolD promoter, domain A of the 35S promoter and the 35S2 promoter. Transgenic Res 4: 388-396.

Pubmed: [Author and Title](#)

Google Scholar: [Author Only Title Only Author and Title](#)

Filichkin SA, Leonard JM, Monteros A, Liu PP, Nonogaki H (2004) A novel endo- β -mannanase associated with anther and gene in tomato LeMAN5 is pollen development. Plant Physiol 134, 1080-1087.

Pubmed: [Author and Title](#)

Google Scholar: [Author Only Title Only Author and Title](#)

Franco-Zorrilla JM, González E, Bustos R, Linhares F, Leyva A, Paz-Ares J (2004) The transcriptional control of plant responses to phosphate limitation. J Exp Bot 55: 285-293.

Pubmed: [Author and Title](#)

Google Scholar: [Author Only Title Only Author and Title](#)

Gaume A, Mächler F, León CD, Narro L, Frossard E (2001) Low-P tolerance by maize (Zea mays L.) genotypes: Significance of root

growth, and organic acids and acid phosphatase root exudation. Plant Soil 228: 253-264.

Pubmed: [Author and Title](#)

Google Scholar: [Author Only Title Only Author and Title](#)

Gu M, Chen A, Sun S, Xu G (2016) Complex regulation of plant phosphate transporters and the gap between molecular mechanisms and practical application: what is missing? Mol Plant 9: 396-416.

Pubmed: [Author and Title](#)

Google Scholar: [Author Only Title Only Author and Title](#)

Guo W, Zhao J, Li X, Qin L, Yan X, Liao H (2011) A soybean β -expansin gene GmEXPB2 intrinsically involved in root system architecture responses to abiotic stresses. Plant J 66: 541-552.

Pubmed: [Author and Title](#)

Google Scholar: [Author Only Title Only Author and Title](#)

Guo WB, Zhang LN, Zhao J, Liao H, Zhuang CX, Yan XL (2008) Identification of temporally and spatially phosphate-starvation responsive genes in Glycine max. Plant Sci 175: 574-584.

Pubmed: [Author and Title](#)

Google Scholar: [Author Only Title Only Author and Title](#)

Gutiérrez-Alanís D, Ojeda-Rivera JO, Yong-Villalobos L, Cárdenas-Torres L, Herrera-Estrella L (2018) Adaptation to phosphate scarcity: tips from Arabidopsis roots. Trends Plant Sci 23: 721-730.

Pubmed: [Author and Title](#)

Google Scholar: [Author Only Title Only Author and Title](#)

Hanifiah FHA, Abdullah SNA, Othman A, Shaharuddin NA, Saud HM, Hasnulhadi HAH, Munusamy U (2018) GCTTCA as a novel motif for regulating mesocarp-specific expression of the oil palm (*Elaeis guineensis* Jacq.) stearoyl-ACP desaturase gene. Plant Cell Rep 37: 1127-1143.

Pubmed: [Author and Title](#)

Google Scholar: [Author Only Title Only Author and Title](#)

Huang KL, Ma GJ, Zhang ML, Xiong H, Wu H, Zhao CZ, Liu CS, Jia HX, Chen L, Kjørven JO, Li XB, Ren F (2018) The ARF7 and ARF19 transcription factors positively regulate PHOSPHATE STARVATION RESPONSE1 in Arabidopsis roots. Plant Physiol 178: 413-427.

Pubmed: [Author and Title](#)

Google Scholar: [Author Only Title Only Author and Title](#)

Ito S, Song YH, Josephson-Day AR, Miller RJ, Breton G, Olmstead RG, Imaizumi T (2012) FLOWERING BHLH transcriptional activators control expression of the photoperiodic flowering regulator CONSTANS in Arabidopsis. PNAS 109: 3582-3587.

Pubmed: [Author and Title](#)

Google Scholar: [Author Only Title Only Author and Title](#)

Jefferson RA (1988) Plant reporter genes: the GUS gene fusion system. Genet Eng 10: 247-263.

Pubmed: [Author and Title](#)

Google Scholar: [Author Only Title Only Author and Title](#)

Jefferson RA, Kavanagh TA, Bevan MW (1987) GUS fusions: β -glucuronidase as a sensitive and versatile gene fusion marker in higher plants. EMBO J 6: 3901-3907.

Pubmed: [Author and Title](#)

Google Scholar: [Author Only Title Only Author and Title](#)

Karthikeyan AS, Ballachanda DN, Raghothama KG (2009) Promoter deletion analysis elucidates the role of cis elements and 5'UTR intron in spatiotemporal regulation of *AtPht1;4* expression in Arabidopsis. Physiol Plant 136: 10-18.

Pubmed: [Author and Title](#)

Google Scholar: [Author Only Title Only Author and Title](#)

Kereszt A, Li D, Indrasumunar A, Nguyen CD, Nontachaiyapoom S, Kinkema M, Gresshoff PM (2007) Agrobacterium rhizogenes-mediated transformation of soybean to study root biology. Nat Protoc 2: 948-952.

Pubmed: [Author and Title](#)

Google Scholar: [Author Only Title Only Author and Title](#)

Kim DW, Lee SH, Choi SB, Won SK, Heo YK, Cho M, Park YI, Cho HT (2006) Functional conservation of a root hair cell-specific cis-element in angiosperms with different root hair distribution patterns. Plant Cell 18: 2958-2970.

Pubmed: [Author and Title](#)

Google Scholar: [Author Only Title Only Author and Title](#)

Kochian LV, Hoekenga OA, Piñeros MA (2004) How do crop plants tolerate acid soils? Mechanisms of aluminum tolerance and phosphorous efficiency. Annu Rev Plant Biol 55: 459-493.

Pubmed: [Author and Title](#)

Google Scholar: [Author Only Title Only Author and Title](#)

Leong SJ, Lu WC, Chiou TJ (2018) Phosphite-mediated suppression of anthocyanin accumulation regulated by mitochondrial atp synthesis and sugars in Arabidopsis. Plant Cell Physiol 59: 1158-1169.

Pubmed: [Author and Title](#)

Google Scholar: [Author Only Title Only Author and Title](#)

Li X, Duan X, Jiang H, Sun Y, Tang Y, Yuan Z, Guo J, Liang W, Chen L, Yin J, Ma H, Wang J, Zhang D (2006) Genome-wide analysis of

basic/helix-loop-helix transcription factor family in rice and Arabidopsis. Plant Physiol 141: 1167-1184.

Pubmed: [Author and Title](#)

Google Scholar: [Author Only Title Only Author and Title](#)

Li X, Zhao J, Tan Z, Zeng R, Liao H (2015) GmEXPB2, a cell wall β -expansin, affects soybean nodulation through modifying root architecture and promoting nodule formation and development. Plant Physiol 169: 2640-2653.

Pubmed: [Author and Title](#)

Google Scholar: [Author Only Title Only Author and Title](#)

Li XH, Wu B, Kong YB, Zhang CY (2014) GmPTF1, a novel transcription factor gene, is involved in conferring soybean tolerance to phosphate starvation. Genet Mol Res 13: 926-937.

Pubmed: [Author and Title](#)

Google Scholar: [Author Only Title Only Author and Title](#)

Li XX, Zeng RS, Liao H (2016) Improving crop nutrient efficiency through root architecture modifications. J Integr Plant Biol 58: 193-202.

Pubmed: [Author and Title](#)

Google Scholar: [Author Only Title Only Author and Title](#)

Li Z, Gao Q, Liu Y, He C, Zhang X, Zhang J (2011) Overexpression of transcription factor ZmPTF1 improves low phosphate tolerance of maize by regulating carbon metabolism and root growth. Planta 233: 1129-1143.

Pubmed: [Author and Title](#)

Google Scholar: [Author Only Title Only Author and Title](#)

Li Z, Liu C, Zhang Y, Wang B, Ran Q, Zhang J (2019) The bHLH family member ZmPTF1 regulates drought tolerance in maize by promoting root development and ABA synthesis. J Exp Bot 70: 5471-5486.

Pubmed: [Author and Title](#)

Google Scholar: [Author Only Title Only Author and Title](#)

Liang CY, Tian J, Liao H (2013) Proteomics dissection of plant responses to mineral nutrient deficiency. Proteomics 13: 624-636.

Pubmed: [Author and Title](#)

Google Scholar: [Author Only Title Only Author and Title](#)

Liang L, Lai Z, Ma W, Zhang Y, Xue Y (2002) AhSL28, a senescence- and phosphate starvation-induced S-like RNase gene in Antirrhinum. Biochim Biophys Acta 1579: 64-71.

Pubmed: [Author and Title](#)

Google Scholar: [Author Only Title Only Author and Title](#)

Massari ME, Murre C (2000) Helix-loop-helix proteins: regulators of transcription in eucaryotic organisms. Mol Cell Biol 20: 429-440.

Pubmed: [Author and Title](#)

Google Scholar: [Author Only Title Only Author and Title](#)

Miura K, Lee J, Gong QQ, Ma SS, Jin JB, Yoo CY, Miura T, Sato A, Bohnert HJ, Hasegawa PM (2011) SIZ1 regulation of phosphate starvation-induced root architecture remodeling involves the control of auxin accumulation. Plant Physiol 155: 1000-1012.

Pubmed: [Author and Title](#)

Google Scholar: [Author Only Title Only Author and Title](#)

Muneer S, Jeong BR (2015) Proteomic analysis provides new insights in phosphorus homeostasis subjected to pi (inorganic phosphate) starvation in tomato plants (Solanum lycopersicum L.). PLOS One 10: e0134103.

Pubmed: [Author and Title](#)

Google Scholar: [Author Only Title Only Author and Title](#)

Neumann G, Martinoia E (2002) Cluster roots -an underground adaptation for survival in extreme environments. Trends Plant Sci 7: 162-167.

Pubmed: [Author and Title](#)

Google Scholar: [Author Only Title Only Author and Title](#)

Oropeza-Aburto A, Cruz-Ramírez A, Acevedo-Hernández GJ, Pérez-Torres CA, Caballero-Pérez J, Herrera-Estrella L (2012) Functional analysis of the Arabidopsis PLDZ2 promoter reveals an evolutionarily conserved low-Pi-responsive transcriptional enhancer element. J Exp Bot 63: 2189-2202.

Pubmed: [Author and Title](#)

Google Scholar: [Author Only Title Only Author and Title](#)

Panigrahy M, Rao DN, Sarla N (2009) Molecular mechanisms in response to phosphate starvation in rice. Biotechnol Adv 27: 389-397.

Pubmed: [Author and Title](#)

Google Scholar: [Author Only Title Only Author and Title](#)

Peng W, Wu W, Peng J, Li J, Lin Y, Wang Y, Tian J, Sun L, Liang C, Liao H (2018) Characterization of the soybean GmALMT family genes and the function of GmALMT5 in response to phosphate starvation. J Integr Plant Biol 60: 216-231.

Pubmed: [Author and Title](#)

Google Scholar: [Author Only Title Only Author and Title](#)

Qin L, Zhao J, Tian J, Chen L, Sun Z, Guo Y, Lu X, Gu M, Xu G, Liao H (2012) The high-affinity phosphate transporter GmPT5 regulates phosphate transport to nodules and nodulation in soybean. Plant Physiol 159: 1634-1643.

Pubmed: [Author and Title](#)

Google Scholar: [Author Only Title Only Author and Title](#)

Rausch C, Bucher M (2002) Molecular mechanisms of phosphate transport in plants. *Planta* 216: 23-37.

Pubmed: [Author and Title](#)

Google Scholar: [Author Only Title Only Author and Title](#)

Rawat R, Xu ZF, Yao KM, Chye ML (2005) Identification of cis-elements for ethylene and circadian regulation of the *Solanum melongena* gene encoding cysteine proteinase. *Plant Mol Biol* 57: 629-643.

Pubmed: [Author and Title](#)

Google Scholar: [Author Only Title Only Author and Title](#)

Rubio-Somoza I, Martinez M, Abraham Z, Diaz I, Carbonero P (2006) Ternary complex formation between HvMYBS3 and other factors involved in transcriptional control in barley seeds. *Plant J* 47: 269-281.

Pubmed: [Author and Title](#)

Google Scholar: [Author Only Title Only Author and Title](#)

Rubio V, Linhares F, Solano R, Martín AC, Iglesias J, Leyva A, Paz-Ares J. 2001. A conserved MYB transcription factor involved in phosphate starvation signaling both in vascular plants and in unicellular algae. *Genes Dev* 15, 2122-2133.

Pubmed: [Author and Title](#)

Google Scholar: [Author Only Title Only Author and Title](#)

Schmidt GW, Delaney SK. 2010. Stable internal reference genes for normalization of real-time RT-PCR in tobacco (*Nicotiana tabacum*) during development and abiotic stress. *Mol Genet Genomics* 283: 233-241.

Pubmed: [Author and Title](#)

Google Scholar: [Author Only Title Only Author and Title](#)

Sharma P, Kumar V, Singh SK, Thakur S, Siwach P, Sreenivasulu Y, Srinivasan R, Bhat SR (2017) Promoter trapping and deletion analysis show *Arabidopsis thaliana* APETALA2 gene promoter is bidirectional and functions as a pollen- and ovule-specific promoter in the reverse orientation. *Appl Biochem Biotechnol* 182: 1591-1604.

Pubmed: [Author and Title](#)

Google Scholar: [Author Only Title Only Author and Title](#)

Simpson SD, Nakashima K, Narusaka Y, Seki M, Shinozaki K, Yamaguchi-Shinozaki K (2003) Two different novel cis-acting elements of *erd1*, a *clpA* homologous *Arabidopsis* gene function in induction by dehydration stress and dark-induced senescence. *Plant J* 33: 259-270.

Pubmed: [Author and Title](#)

Google Scholar: [Author Only Title Only Author and Title](#)

Stougaard J, Jorgensen JE, Christensen T, Kuhle A, Marcker KA (1990) Interdependence and nodule specificity of cis-acting regulatory elements in the soybean leghemoglobin *lbc3* and *N23* gene promoters. *Mol Gen Genet* 220: 353-360.

Pubmed: [Author and Title](#)

Google Scholar: [Author Only Title Only Author and Title](#)

Suen DF, Tsai YH, Cheng YT, Radjacomare R, Ahirwar RN, Fu H, Schmidt W (2018) The deubiquitinase OTU5 regulates root responses to phosphate starvation. *Plant Physiol* 176: 2441-2455.

Pubmed: [Author and Title](#)

Google Scholar: [Author Only Title Only Author and Title](#)

Sun LC, Song L, Zhang Y, Zheng Z, Liu D (2016) *Arabidopsis* PHL2 and PHR1 act redundantly as the key components of the central regulatory system controlling transcriptional responses to phosphate starvation. *Plant Physiol* 170: 499-514.

Pubmed: [Author and Title](#)

Google Scholar: [Author Only Title Only Author and Title](#)

Tian J, Wang X, Tong Y, Chen X, Liao H (2012) Bioengineering and management for efficient phosphorus utilization in crops and pastures. *Curr Opin Biotechnol* 23: 866-871.

Pubmed: [Author and Title](#)

Google Scholar: [Author Only Title Only Author and Title](#)

Tian J, Wang C, Zhang Q, He X, Whelan J, Shou H (2014) Overexpression of OsPAP10a, a root-associated acid phosphatase, increased extracellular organic phosphorus utilization in rice. *J Integr Plant Biol* 54: 631-639.

Pubmed: [Author and Title](#)

Google Scholar: [Author Only Title Only Author and Title](#)

Timerbaev V, Dolgov S (2019) Functional characterization of a strong promoter of the early light-inducible protein gene from tomato. *Planta* 250: 1307-1323.

Pubmed: [Author and Title](#)

Google Scholar: [Author Only Title Only Author and Title](#)

Toledo-Ortiz G, Huq E, Quail PH (2003) The *Arabidopsis* basic/helix-loop-helix transcription factor family. *Plant Cell* 15: 1749-1770.

Pubmed: [Author and Title](#)

Google Scholar: [Author Only Title Only Author and Title](#)

Urao T, Yamaguchi-Shinozaki K, Urao S, Shinozaki K (1993) An *Arabidopsis* myb homolog is induced by dehydration stress and its gene product binds to the conserved MYB recognition sequence. *Plant Cell* 5: 1529-1539.

Pubmed: [Author and Title](#)

Google Scholar: [Author Only Title Only Author and Title](#)

Wang D, Lv S, Jiang P, Li Y (2017) Roles, regulation, and agricultural application of plant phosphate transporters. Front Plant Sci 8: 817.

Pubmed: [Author and Title](#)

Google Scholar: [Author Only Title Only Author and Title](#)

Wang L, Zeng JH, Song J, Feng SJ, Yang ZM (2015) miRNA778 and SUVH6 are involved in phosphate homeostasis in Arabidopsis. Plant Sci 238, 273-285.

Pubmed: [Author and Title](#)

Google Scholar: [Author Only Title Only Author and Title](#)

Wang X, Wang Y, Tian J, Lim BL, Yan X, Liao H (2009) Overexpressing AtPAP15 enhances phosphorus efficiency in soybean. Plant Physiol 151: 233-240.

Pubmed: [Author and Title](#)

Google Scholar: [Author Only Title Only Author and Title](#)

Williamson LC, Ribrioux SPCP, Fitter AH, Ottoline Leyser HM (2001) Phosphate availability regulates root system architecture in Arabidopsis. Plant Physiol 126: 875-882.

Pubmed: [Author and Title](#)

Google Scholar: [Author Only Title Only Author and Title](#)

Wray GA, Hahn MW, Abouheif E, Balhoff JP, Pizer M, Rockman MV, Romano LA (2003) The evolution of transcriptional regulation in eukaryotes. Mol Biol Evol 20: 1377-1419.

Pubmed: [Author and Title](#)

Google Scholar: [Author Only Title Only Author and Title](#)

Wu P, Wang X (2008) Role of OsPHR2 on phosphorus homeostasis and root hairs development in rice (Oryza sativa L.). Plant Signal Behav 3: 674-675.

Pubmed: [Author and Title](#)

Google Scholar: [Author Only Title Only Author and Title](#)

Xue YB, Xiao BX, Zhu SN, Mo XH, Liang CY, Tian J, Liao H (2017) GmPHR25, a GmPHR member up-regulated by phosphate starvation, controls phosphate homeostasis in soybean. J Exp Bot 68: 4951-4967.

Pubmed: [Author and Title](#)

Google Scholar: [Author Only Title Only Author and Title](#)

Yang WT, Baek D, Yun DJ, Lee KS, Hong SY, Bae KD, Chung YS, Kwon YS, Kim DH, Jung KH, Kim DH (2018) Rice OsMYB5P improves plant phosphate acquisition by regulation of phosphate transporter. PLOS One 13: e0194628.

Pubmed: [Author and Title](#)

Google Scholar: [Author Only Title Only Author and Title](#)

Yi K, Wu Z, Zhou J, Du L, Guo L, Wu Y, Wu P (2005) OsPTF1, a novel transcription factor involved in tolerance to phosphate starvation in rice. Plant Physiol 138: 2087-2096.

Pubmed: [Author and Title](#)

Google Scholar: [Author Only Title Only Author and Title](#)

Zhang H, Jing R, Mao X (2017) Functional characterization of TaSnRK2.8 promoter in response to abiotic stresses by deletion analysis in transgenic Arabidopsis. Front Plant Sci 8: 1198.

Pubmed: [Author and Title](#)

Google Scholar: [Author Only Title Only Author and Title](#)

Zhao J, Fu JB, Liao H, He Y, Nian H, Hu YM, Qiu LJ, Dong YS, Yan XL (2004) Characterization of root architecture in an applied core collection for phosphorus efficiency of soybean germplasm. Chinese Sci Bull 49: 1611-1620.

Pubmed: [Author and Title](#)

Google Scholar: [Author Only Title Only Author and Title](#)

Zhou DX (1999) Regulatory mechanism of plant gene transcription by GT-elements and GT-factors. Trends Plant Sci 4: 210-214.

Pubmed: [Author and Title](#)

Google Scholar: [Author Only Title Only Author and Title](#)

Zhou J, Xie J, Liao H, Wang X (2014) Overexpression of β -expansin gene GmEXPB2 improves phosphorus efficiency in soybean. Physiol Plant 150: 194-204.

Pubmed: [Author and Title](#)

Google Scholar: [Author Only Title Only Author and Title](#)

Zhou K, Yamagishi M, Osaki M, Masuda K (2008) Sugar signalling mediates cluster root formation and phosphorus starvation-induced gene expression in white lupin. J Exp Bot 59: 2749-2756.

Pubmed: [Author and Title](#)

Google Scholar: [Author Only Title Only Author and Title](#)